VNU Journal of Science: Mathematics - Physics

Journal homepage: https://js.vnu.edu.vn/MaP

Preparation and Characterization of Quantum Dots Sensitized Solar Cells Based on TiO_2/CdS:Mn^{2+}/CdSe Photoanode

Ha Thanh Tung[1,*], Nguyen Cong Hau[2], Nguyen Tan Phat[3], Lam Quang Vinh[4]

[1]Faculty of Physics, DongThap University, Dong Thap Province, Vietnam
[2]University of Science, VNU-HCM, Vietnam
[3]Department of Physics, HCMC University of Education, Vietnam
[4]Vietnam National University - HCM City, Vietnam

Abstract: In this study, we have prepared and investigated the optical properties of the TiO_2/CdS:Mn^{2+}/CdSe photoanode as the function of Mn^{2+} doping concentration and thickness. The results show that the peaks of the UV-Vis spectra shifted toward longer wavelength while Mn^{2+} doping concentrations or thickness of the films were changed. The main cause of the red-shifting in UV-Vis spectra may come from the increasing of photoanode light-harvesting capacity. In addition, the results also demonstrated by the boosting performance of quantum dots sensitized solar cells from 2.07% for TiO_2/CdS/CdSe photoanode to 2.5% for TiO_2/CdS:Mn^{2+}/CdSe photoanode.

Keywords: Solar cells, nano CdS, nano CdSe.

1. Introduction

Quantum dots sensitized solar cells (QDSSCs) can be regarded as a derivative of dye sensitized solar cells (DSSCs) by replacing dye molecules with quantum dots (QDs). QDs have been chosen as a main photosensitizer in solar cells since they have several optical and electrical advantages, including: tunable band gap depending on the QD size due to the quantum confinement effect, higher absorption coefficient than most organic dyes, and multiple exciton generation (MEG) effect [1-3]. Moreover, QDs can generate multiple electron-hole pairs from a single incident photon absorption (MEG), which allowed the power conversion efficiency (PCE) of QDSSCs overcome the Shockley – Queisser limit of traditional Si solar cells. Therefore, QDSSC is expected to create a great potential for breakthrough

efficiency [4]. First considerable research in this field belonged to Vogel and coworkers on nanocrystal CdS QDSSCs, despite of very low PCE. Until 2008, most of researched QDSSCs still used only single QD so the light absorbing domain is limited and the efficiency cannot be improved. Thereafter, several researches had been focused on enhancing the QDSSCs PCE, such as: extending the photoanode absorption [2-6]; using several photoanode preparation methods: chemical bath deposition (CBD), successive ionic layer absorption and reaction (SILAR), etc… [7]; applying the core-shell structure to improve the recombination process of QDs surface traps and the electron injection into TiO_2 [8]; using the linkers of TiO_2 and QDs [9-10]. However, high PCE of QDSSCs has been not archived until now. Recently, Tubtimtae et.al. reported the PCE of QDSSCs reached 3.1% [11]. Therefore, multiple problems need to be researched on applying QDs to solar cell, including: (1) synthesis QDs having compatible electrical and optical properties; (2) the optimum binding of QDs and TiO_2; (3) optimal surface trap-states treatment methods to increasing the QDs stability in electrolyte [12-13]; (4) preparing QDSSCs with tandem structure to extend the light absorption domain (from ultraviolet to near-infrared region) for enhancing the QDSSCs PCE [4-6, 14-15]. Some researchers had been conducted recently on doping transitional metal ions into pure QDs, such as PbS nanocrystal doping Hg^{2+} [8] and $CdSe:Cu^{2+}$ [11]. The appearance of a dopant energy level in the band gap of pure QDs increases the photon absorption capacity and then enhances the current density of QDSSCs [10-11]. Therefore, doping transitional metal ions into pure QDs is an effective method for improving the PCE of QDSSCs.

In this research, we doped ions Mn^{2+} into pure CdS nanocrystals of $TiO_2/CdS:Mn^{2+}/CdSe$ photoanode and the optical properties of the photoanode have been investigated by the function of ion doping concentration and layer thickness. Finally, we fabricated the QDSSCs based on the optimal photoanode.

2. Materials and methods

2.1. Photoanode preparation

Preparation of mesoporous TiO_2 films: FTO glass substrates (Dyesol, TEC15, 1.4x2.1cm) were prepared by following steps: ultrasonic cleaning in soap solution for 30mins followed with deep washing in pure water and ethanol; dipping in 40mM $TiCl_4$ solution at $70°C$ in 30mins then washing with deionized water and drying before using. Mesoporous TiO_2 films were prepared onto cleaned FTO substrates via doctor-blading method followed with sintered at $500°C$ for 30mins.

Preparation of $TiO_2/CdS:Mn^{2+}$ photoanodes: Prepared TiO_2 films were immersed into the mixture of Cd^{2+} and Mn^{2+} ionized solution for 5mins at room temperature, then rinsed with ethanol to remove excess precursors and dried before the next dipping. The films were next dipped into S^{2-} solution for 5mins at room temperature followed with rising by methanol and drying. These steps are called one SILAR cycle. This process was repeated from 1 to 5 times.

Preparation of $TiO_2/CdS:Mn^{2+}/CdSe$ photoanodes: The $TiO_2/CdS:Mn^{2+}/CdSe$ photoanodes were prepared similarly as described above. Briefly, the $TiO_2/CdS:Mn^{2+}$ layers were immersed into Cd^{2+} ionized solution for 5mins at room temperature, then rinsed with ethanol to remove excess precursors and dried. The films were next dipped into Se^{2-} solution for 5mins at room temperature followed by rinsing by methanol and drying. This cycle was repeated 3 times.

Preparation of QDSSCs: The polysulfide electrolyte was prepared by dissolving 0.5 $Na_2S.9H_2O$, 0.2M S and 0.2M KCl in the mixture of deionized water and methanol solution (ratio 7:3 in volume). For the Pt cathode preparation, commercial Pt paste were doctor-bladed onto cleaned FTO glass

substrates then sintered at $500°C$ for 30mins. Completed QDSSCs consisted of photoanode and counter electrode adhesive by surlyn layer heated at $170°C$.
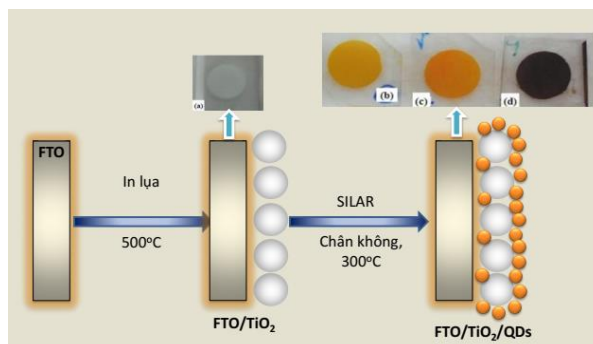

Figure 1. Schematic of the photoanode $TiO_2/CdS:Mn^{2+}/CdSe$ preparation.

2.2. Measurement

Field-effect scanning electron microscope (FESEM) of Ho Chi Minh City Institute of Physics was used to investigate the surface morphology and composition of the photoanode. The UV-Vis spectra was characterized by the JASCO V-670 device of Applied Physical Chemistry lab of University of Science, Vietnam National University – Ho Chi Minh City. X-ray diffraction (XRD) spectra and photocurrent-voltage (I-V) curves were analyzed by devices of two aforementioned offices.

3. Results and discussion

TiO_2 plays the role of intermediate layer for QDs assembling. The thicker the layer was the more QDs assembled. However, the thickness of TiO_2 layer had been optimal since the decreasing of PCE and the increasing of internal resistance of QDSSCs when the thickness of TiO_2 layer increased. The transmittance of photoanode with a different TiO_2 layer had been investigated. In Fig. 2a, the photoanode included single TiO_2 layer was inequality and limited, which leads to the transmittance of TiO_2 layer was equivalent with FTO substrate. When the amount of TiO_2 layer was more than 3, the optical properties of photoanode was declined since the decreasing of transmittance and the quality of the electrode. Therefore, two layers of TiO_2 were prepared on FTO for QDs assembling.
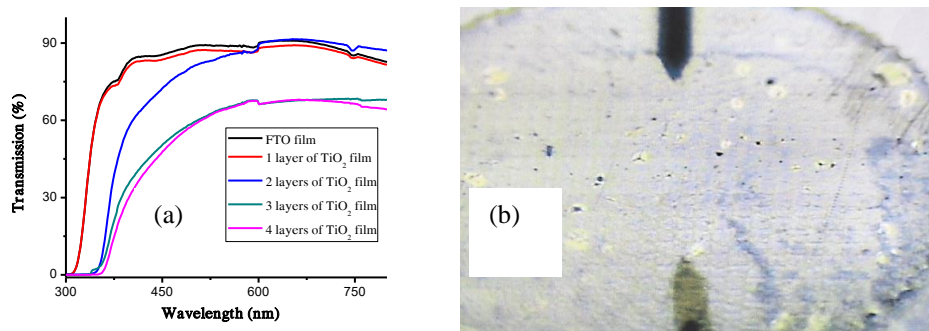

Figure 2. (a) The transmittance of electrode with different number of TiO_2 doctor-bladed layer and (b) the thickness of TiO_2 layer measured by stylus.

Stylus had been carried out for measuring the thickness of TiO_2 layer and the results were approximately 11-12μm (Fig. 2b)
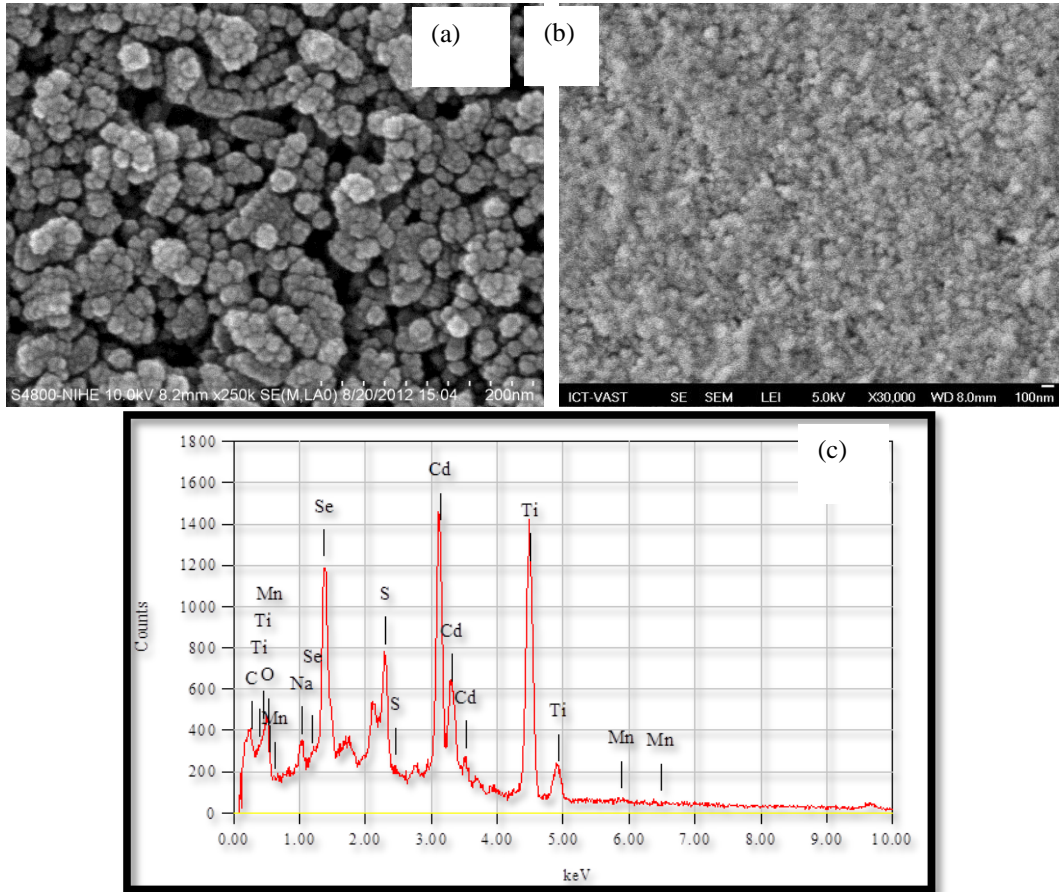

Figure 3. FE-SEM image of (a) TiO_2 and TiO_2/CdS:Mn^{2+}/CdSe film, (c) EDX of TiO_2/CdS:Mn^{2+}/CdSe film.

The surface morphology of the photoanode had been investigated. The FESEM image of TiO_2/CdS:Mn^{2+}/CdSe photoanode at 100nm resolution was demonstrated (Fig. 3b). The layer had high porosity, the average dimension of nanoparticles was a few dozen of nanometers. Because of huge size TiO_2 nanoparticles (Fig. 3a), the layer had high porosity and there were more spaces between particles, which lead to the higher assembled ability of CdS:Mn^{2+} and CdSe QDs onto the surface of TiO_2 nanoparticles. There are two main problems which had been investigated for applying the photoanode for QDSSCs, including: (1) QDs had been assembled on the surfaces of TiO_2 nanoparticles instead of sticking on the layer; (2) the concentration of assembled QDs onto TiO_2 layer could not form bulk morphology.

The energy peaks related to Ti and O element in TiO_2 were clearly founded in the energy dispersive X-ray (EDX) spectra of TiO_2/CdS:Mn^{2+}/CdSe photoanode. Cd, Se, and S – energy peaks were also illustrated in the spectra, corresponded to the composition of CdS and CdSe nanocrystal. Si and C – energy peaks had been originated from FTO and excessive organic solution remaining in the layer (since the electrodes were sintered in vacuum), respectively. Mn – energy peaks came from the

anion precursor solution. The EDX spectra confirmed that QDs had been assembled and crystallized on the TiO_2 layer (Fig. 3c and Table 1).

Table 1. EDX quantitative analysis of $TiO_2/CdS:Mn^{2+}/CdSe$ photoanode

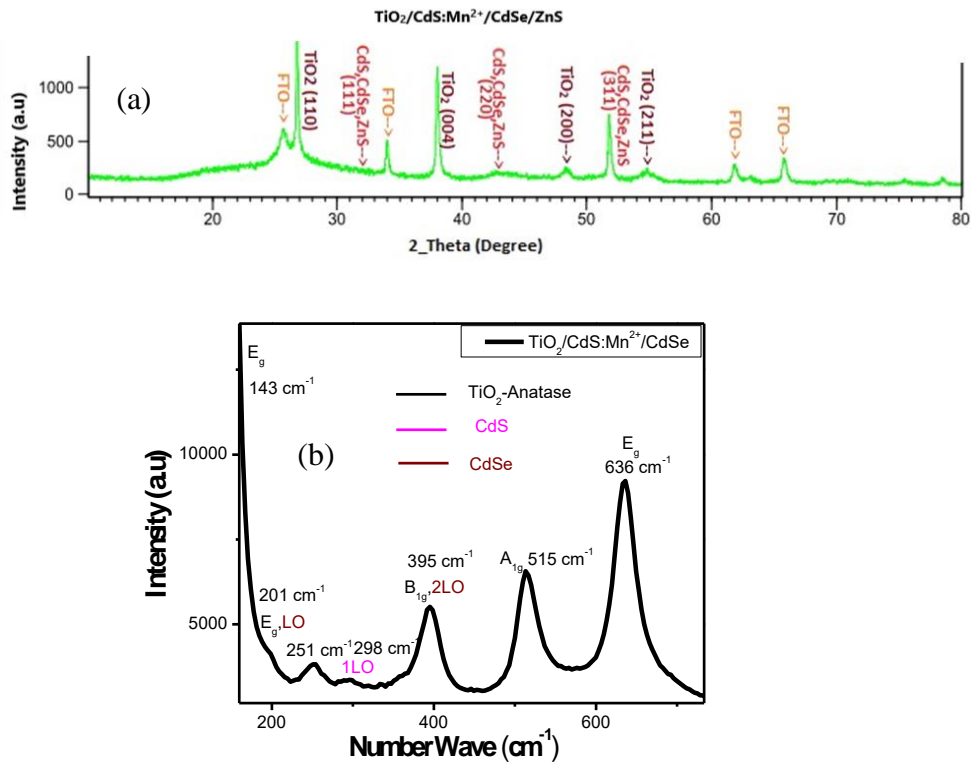| Elements (k)	Energy (KeV)	Ratio of mass (%)	Error (%)	Ratio of Atom (%)
C	0.277	1.54	0.06	8.21
O	0.525	0.97	0.14	3.90
Na	1.041	0.68	0.26	1.91
Si	1.739	0.43	0.59	0.98
S	2.307	4.92	0.05	9.84
Ti	4.508	23.25	0.02	31.12
Mn	5.894	0.52	1.87	0.60
Se	1.379	20.08	0.04	16.30
Cd	3.133	47.06	0.02	27.16
Total		100.00		100.00

Figure 4. (a) X-ray diffraction (XRD) and (b) Raman scattering spectra of $TiO_2/CdS:Mn^{2+}/CdSe$ photoanode

As can be seen in Fig 4a, it is immediately obvious that the XRD of $TiO_2/CdS:Mn^{2+}/CdSe/ZnS$ appears the peaks at $32°$, $43.1°$ and $52°$ positions corresponding to the (111), (220) and (311) planes, which indicates an upstanding CdS, CdSe and ZnS zinc Blende. It is a completely suitable result for JCPDS No. 05-5666, JCPDS No. 88-2346, JCPDS No. 41-1019, respectively. Moreover, the left peaks of XRD pattern can be assigned the TiO_2 anatase (JCPDS No. 21-1272). This implies that $CdS:Mn^{2+}$, CdSe and ZnS nanoparticles have absorbed on TiO_2 films. These results were also affirmative through

Raman scattering spectra of same components photoanode (Fig. 4b). The oscillated mode at 143cm^{-1}, 251cm^{-1}, 515cm^{-1}, and 636cm^{-1} featured for the anatase-phase of TiO_2 nanoparticle and the others at 201cm^{-1}, 298cm^{-1} and 395cm^{-1} corresponded to cube CdS:Mn^{2+} and CdSe nanocrystal.
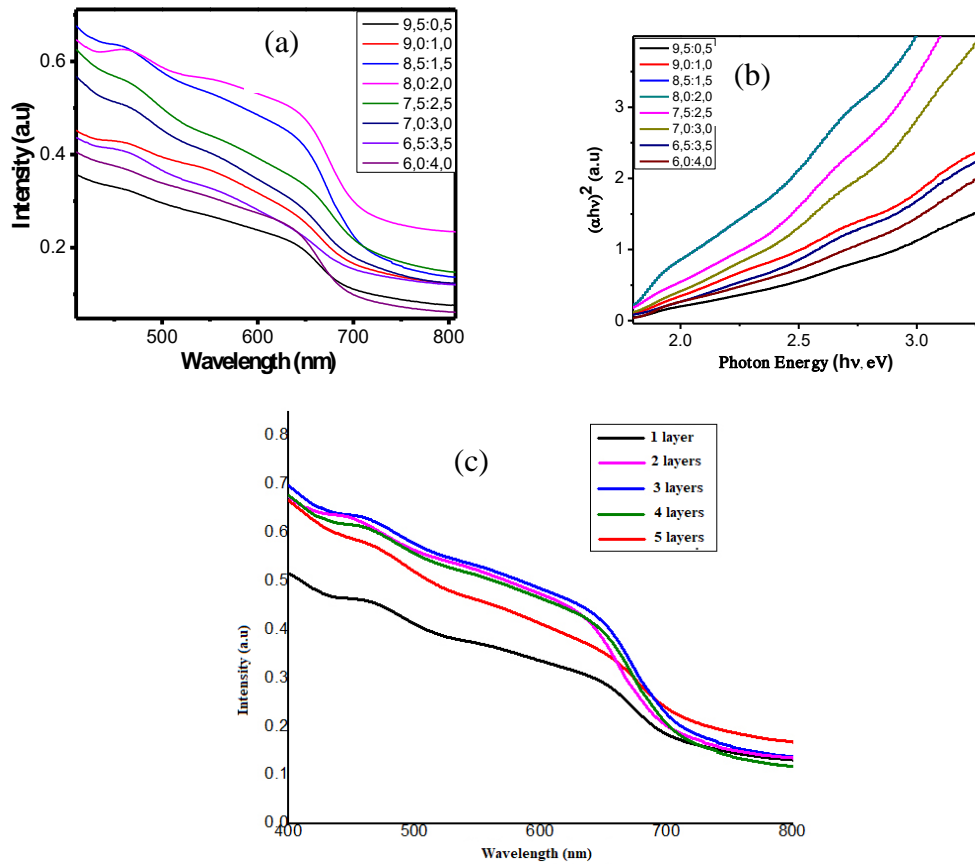

Figure 5. (a) UV-Vis spectra and (b) inferred $(\alpha h\nu)^2$ versus (hν) curves of TiO_2/CdS:Mn^{2+}/CdSe photoanode at different Cd:Mn ratio; (c) UV-Vis spectra of photoanode at different thickness.

The UV-Vis spectra of prepared TiO_2/CdS:Mn^{2+}/CdSe photoanode with 3 SILAR cycles of CdS:Mn^{2+} and CdSe nanocrystal had been investigated in the wavelength region from 300 to 850nm (Fig. 5a). Because of a large band gap energy (3.2eV in bulk), TiO_2 nanoparticles absorbed weakly in the visible domain. The absorption edge of TiO_2/CdS photoanode was at approximately 460nm corresponded to the significant absorption region of CdS nanocrystal, which were mentioned in other publications [16, 17]. When ion Mn^{2+} were doped into CdS nanocrystal and the CdSe QDs were assembled, the photoanode absorbance increased significantly and the absorption edge shifted to a approximately 620nm region at the ratio of Cd:Mn = 8:2. The intensity and position of absorption peaks were slightly different at others ratio Cd:Mn.

The relationship between the absorbance (α) and the incident photon energy (hν) in UV-Vis spectra in the strong absorption region of semiconductors can be derived by Tauc equation [18]

$$\alpha h\nu = \alpha_0 \left(h\nu - E_g \right)^n \tag{1}$$

With α_0 is an independent constant with incident photon energy and E_g is the semiconductor band gap energy. The constant n in the equation (1) was the power factor of the optical transitions in the semiconductor, depend on these transitions and structure of semiconductor (amorphous or crystal). This constant can be 1/2, 2, 3/2, or 3 depending on the nature of semiconductor [18]. By plotting all the curves illustrated the relationship between the absorbance (α) and the incident photon energy (hν) of TiO$_2$/CdS and TiO$_2$/CdS/CdSe photoanode with all possible value of n, the most accordant and fully symmetric curve was at n = 1/2. As can be seen in Fig. 5b, there was a linear region in the relationship between $(\alpha h\nu)^2$ and incident photon energy (hν). The effective band gap can be estimated by extrapolating the linear portion. The band gap energy of TiO$_2$/CdS:Mn^{2+}/CdSe nanocrystal with ion Mn^{2+} doping concentration varied from 5% to 40% were 1.93eV, 1.91eV, 1.90eV, 1.89eV, 1.88eV, 1.91eV, 1.92eV and 1,90eV, respectively. These values are larger than 1.7eV of CdSe band gap energy in bulk [18], indicated that synthesized particles were in nanoscale.

Besides Cd:Mn ratio, the number of SILAR cycle of the CdS:Mn^{2+} nanocrystal synthesis was also an important factor determined the crystal properties. The higher the SILAR cycle was the greater the nanocrystal was and the smaller the bandgap energy of semiconductor was. Since the photoanode need to be in tandem structure, the amount of SILAR cycle had been optimal. The optical properties of CdS:Mn^{2+} nanocrystal at different SILAR cycle from 1 to 5 had been investigated by UV-Vis spectra of TiO$_2$/CdS:Mn^{2+}/CdSe photoanode.

The UV-Vis spectra of TiO$_2$/CdS:Mn^{2+}/CdSe photoanode was illustrated in Fig. 5c. When the SILAR cycle increased from 1 to 3 cycles, the absorption edges were red-shifted, obviously from 610 to 620nm region and the absorbance increased rapidly. The energy band gap of the semiconductor decreased when the dimension of particles increased was the possible reason for the changing in UV-Vis spectra. At 4 and 5 SILAR cycles, the red-shift of absorption edge was changed insignificantly compared to 3 SILAR cycles since the crystal dimension reached a saturation state and the gap space between TiO$_2$ nanoparticles were fully filled by CdS:Mn^{2+} nanocrystal [19-21].

Table 2. Photovoltaic parameters obtained from I-V curves of QDSSCs with different Cd:Mn ratio

Cd:Mn	Absorption peak (nm)	Band gap (eV)	FF	J_{SC}(mA/cm^2)	V_{OC}(V)	η(%)
9,5:0,5	644	1,93	0,291	7,780	0,417	0,947
9,0:1,0	648	1,91	0,348	7,738	0,411	1,110
8,5:1,5	651	1,90	0,347	12,008	0,460	1,990
8,0:2,0	657	1,89	0,34	12,5	0,49	2,5
7,5:2,5	658	1,88	0,341	11,520	0,476	1,876
7,0:3,0	650	1,91	0,374	9,566	0,458	1,619
6,5:3,5	646	1,92	0,325	9,230	0,442	1,332
6,0:4,0	651	1,90	0,346	8,617	0,430	1,285

Table 3. Photovoltaic parameters obtained from I-V curves of QDSSCs with different thickness layers

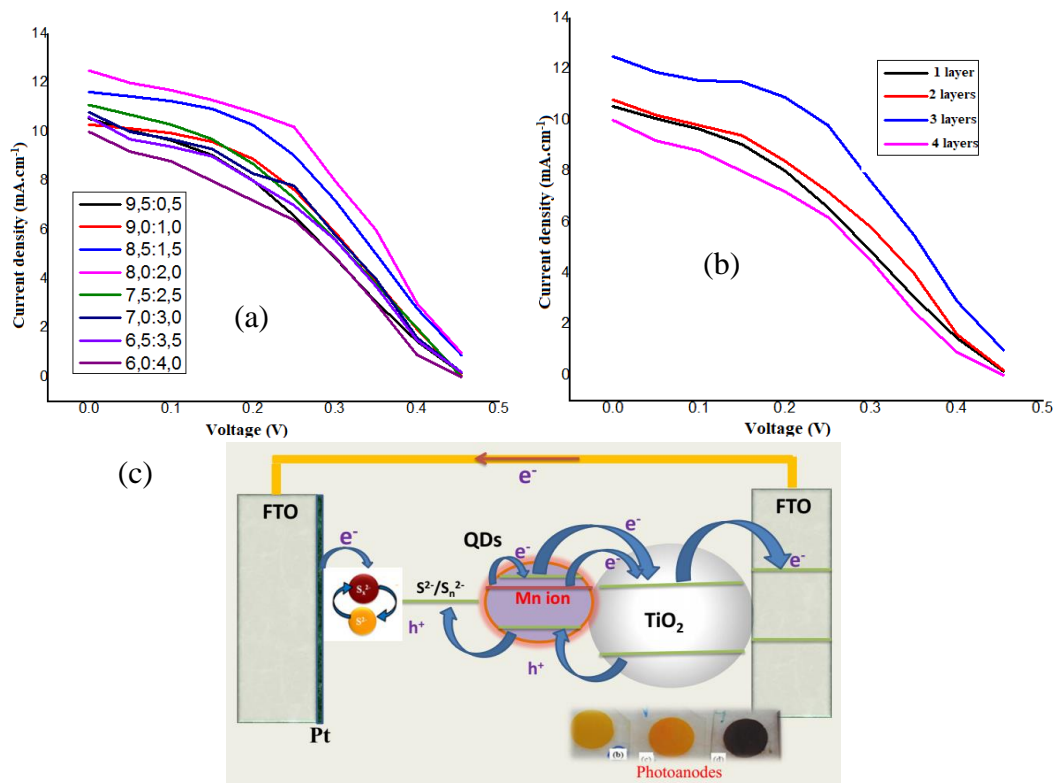| Photoanodes	FF	J_{SC}(mA/cm^2)	V_{OC}(V)	η(%)
TiO$_2$/CdS:Mn^{2+}(1)/CdSe(3)	0,529	5,425	0,430	1,398
TiO$_2$/CdS:Mn^{2+}(2)/CdSe(3)	0,420	9,070	0,466	1,747
TiO$_2$/CdS:Mn^{2+}(3)/CdSe(3)	0,34	12,5	0,49	2,5
TiO$_2$/CdS:Mn^{2+}(4)/CdSe(3)	0,451	8,690	0,489	1,910
TiO$_2$/CdS:Mn^{2+}(5)/CdSe(3)	0,434	7,990	0,4644	1,612

Figure 6. I-V curves of QDSSCs in the function of (a) Cd:Mn ratio and (b) thickness layer;
(c) structure diagram of QDSSCs.

The PCE of QDSSCs using pure CdS nanocrystal was 1.52%. When ion Mn^{2+} were doped, photovoltaic parameters of QDSSCs enhanced significantly. At 20% ion Mn^{2+} doping concentration, the short-circuit current density, open-voltage and fill factor were $J_{SC} = 12,5 mA/cm^2$, $V_{OC} = 0.49V$, and $FF = 0.34$, respectively, and the PCE of QDSSCs reached 2.5%. The enhancing of photovoltaic parameters and PCE of doped QDSSCs can be came from these possible reasons: (1) the doped photoanode had higher absorbance and could generate more excited electrons; (2) the absorption edge of $CdS:Mn^{2+}$ photoanode shifted towards longer wavelength (red-shift) so more photons in the visible region can be absorbed; (3) ion Mn^{2+} generated an intermediate energy level in the band gap of CdS nanocrystal so incident photons which had energy smaller than semiconductor band gap can be absorbed then generated more excited electrons, as was demonstrated by the enhancing of the short-circuit current density of doped QDSSCs compared to undoped cells. Thus, doping ion Mn^{2+} into CdS nanocrystal plays an important role in improving the PCE of QDSSCs.

The photovoltaic parameters and PCE of QDSSCs were enhanced significantly when the ion Mn^{2+} doping concentration increased from 0.1 to 0.2. Specifically, QDSSCs included photoanode with 20% ion Mn^{2+} doping concentration reached the PCE of 2.5% (increased 164% to undoped QDSSCs) with the short-circuit current density, open-voltage and fill factor were $J_{SC} = 12.5 mA/cm^2$, $V_{OC} = 0.49V$, and $FF = 0.34$, respectively. More excited electrons were generated since the absorbance of photoanode increased (at 20% ion Mn^{2+} doping concentration, the photoanode had highest absorption as illustrated in Fig. 5a) accompanied by a tandem structure in the energy level of photoanode which facilitated carrier diffusion, lead to the increasing of the short-circuit current density and PCE of QDSSCs.

However, the photovoltaic parameters and PCE of QDSSCs decreased when the doping concentration overcame 0.2. The PCE reached 2.5% and 1.227% at 20% and 50% Mn^{2+} ion doping concentration, respectively. This reduction can be explained by the decreasing of photoanode absorbance at 50% compared to 20% doped photoanode, which lead to the decline of excited electron generation. From this result, it can be inferred that the PCE of QDSSCs would be decreased if ion Mn^{2+} doping concentration continued increasing since the CdS nanocrystal lattice reached the saturation state [22].

4. Conclusions

We successfully fabricated QDSSCs with TiO_2/CdS:Mn^{2+}/CdSe photoanode with different ion Mn^{2+} doping concentration and CdS:Mn^{2+} thickness layer. By optimizing preparation parameters, the PCE of QDSSCs reached a value as large as 2.5% at 20% doping concentration and the number of CdS:Mn^{2+} SILAR cycle was 3.

Acknowledgements

References

[1] Kamat, Prashant V. "Quantum dot solar cells. Semiconductor nanocrystals as light harvesters." The Journal of Physical Chemistry C 112, no. 48 (2008): 18737-18753.

[2] González-Pedro, Victoria, Xueqing Xu, Iván Mora-Sero, and Juan Bisquert. "Modeling high-efficiency quantum dot sensitized solar cells." ACS nano 4, no. 10 (2010): 5783-5790. Tian, Jianjun, and Guozhong Cao. "Control of nanostructures and interfaces of metal oxide semiconductors for quantum-dots-sensitized solar cells." The journal of physical chemistry letters 6, no. 10 (2015): 1859-1869.

[3] Beard, Matthew C., Aaron G. Midgett, Mark C. Hanna, Joseph M. Luther, Barbara K. Hughes, and Arthur J. Nozik. "Comparing multiple exciton generation in quantum dots to impact ionization in bulk semiconductors: implications for enhancement of solar energy conversion." Nano letters 10, no. 8 (2010): 3019-3027.

[4] Lopez-Luke, Tzarara, Abraham Wolcott, Li-ping Xu, Shaowei Chen, Zhenhai Wen, Jinghong Li, Elder De La Rosa, and Jin Z. Zhang. "Nitrogen-doped and CdSe quantum-dot-sensitized nanocrystalline TiO2 films for solar energy conversion applications." The Journal of Physical Chemistry C 112, no. 4 (2008): 1282-1292.

[5] Mora-Seró, Iván, Sixto Giménez, Thomas Moehl, Francisco Fabregat-Santiago, Teresa Lana-Villareal, Roberto Gómez, and Juan Bisquert. "Factors determining the photovoltaic performance of a CdSe quantum dot sensitized solar cell: the role of the linker molecule and of the counter electrode." Nanotechnology 19, no. 42 (2008): 424007.

[6] Shen, Qing, Junya Kobayashi, Lina J. Diguna, and Taro Toyoda. "Effect of ZnS coating on the photovoltaic properties of CdSe quantum dot-sensitized solar cells." Journal of Applied Physics 103, no. 8 (2008): 084304.

[7] Lee, Jin-Wook, Dae-Yong Son, Tae Kyu Ahn, Hee-Won Shin, In Young Kim, Seong-Ju Hwang, Min Jae Ko, Soohwan Sul, Hyouksoo Han, and Nam-Gyu Park. "Quantum-dot-sensitized solar cell with unprecedentedly high photocurrent." Scientific reports 3 (2013): 1050.

[8] Santra, Pralay K., and Prashant V. Kamat. "Mn-doped quantum dot sensitized solar cells: a strategy to boost efficiency over 5%." Journal of the American Chemical Society 134, no. 5 (2012): 2508-2511.

[9]   Zhu, Guang, Likun Pan, Tao Xu, and Zhuo Sun. "CdS/CdSe-cosensitized TiO2 photoanode for quantum-dot-sensitized solar cells by a microwave-assisted chemical bath deposition method." ACS applied materials & interfaces 3, no. 8 (2011): 3146-3151.

[10] Lee, Yong Hui, Sang Hyuk Im, Jeong Ah Chang, Jong-Heun Lee, and Sang Il Seok. "CdSe-sensitized inorganic–organic heterojunction solar cells: the effect of molecular dipole interface modification and surface passivation." Organic Electronics 13, no. 6 (2012): 975-979.

[11] Hossain, Md Anower, James Robert Jennings, Chao Shen, Jia Hong Pan, Zhen Yu Koh, Nripan Mathews, and Qing Wang. "CdSe-sensitized mesoscopic TiO 2 solar cells exhibiting> 5% efficiency: redundancy of CdS buffer layer." Journal of Materials Chemistry 22, no. 32 (2012): 16235-16242.

[12] Wang, Jin, Iván Mora-Seró, Zhenxiao Pan, Ke Zhao, Hua Zhang, Yaoyu Feng, Guang Yang, Xinhua Zhong, and Juan Bisquert. "Core/shell colloidal quantum dot exciplex states for the development of highly efficient quantum-dot-sensitized solar cells." Journal of the American Chemical Society 135, no. 42 (2013): 15913-15922.

[13] Radich, James G., Nevin R. Peeples, Pralay K. Santra, and Prashant V. Kamat. "Charge transfer mediation through Cu x S. The hole story of CdSe in polysulfide." The Journal of Physical Chemistry C 118, no. 30 (2014): 16463-16471.

[14] Wang, Jin, Iván Mora-Seró, Zhenxiao Pan, Ke Zhao, Hua Zhang, Yaoyu Feng, Guang Yang, Xinhua Zhong, and Juan Bisquert. "Core/shell colloidal quantum dot exciplex states for the development of highly efficient quantum-dot-sensitized solar cells." Journal of the American Chemical Society 135, no. 42 (2013): 15913-15922.

[15] Yan, Keyou, Lixia Zhang, Jianhang Qiu, Yongcai Qiu, Zonglong Zhu, Jiannong Wang, and Shihe Yang. "A quasi-quantum well sensitized solar cell with accelerated charge separation and collection." Journal of the American Chemical Society 135, no. 25 (2013): 9531-9539.

[16] Q. Dai, E. M. Sabio, W. Wang and J. Tang, Appl. Phys. Lett.,2014, 104. 183901. 32. T. Debnath, P. Maity, S. Maiti and H. N. Ghosh, J. Phys. Chem.Lett., 2014, 5, 2836-2842.

[17] Lee, Yuh-Lang, and Yi-Siou Lo. "Highly efficient quantum-dot-sensitized solar cell based on co-sensitization of CdS/CdSe." Advanced Functional Materials 19, no. 4 (2009): 604-609.

[18] Xie, Yu-Long. "Enhanced photovoltaic performance of hybrid solar cell using highly oriented CdS/CdSe-modified TiO2 nanorods." Electrochimica Acta 105 (2013): 137-141.

[19] Xing, Chanjuan, Yaojun Zhang, Wei Yan, and Liejin Guo. "Band structure-controlled solid solution of Cd1-x ZnxS photocatalyst for hydrogen production by water splitting." International Journal of Hydrogen Energy 31, no. 14 (2006): 2018-2024.

[20] Askari, Mina, Nayereh Soltani, Elias Saion, W. Mahmood Mat Yunus, H. Maryam Erfani, and Mahdi Dorostkar. "Structural and optical properties of PVP-capped nanocrystalline $Zn_xCd_{1-x}S$ solid solutions." Superlattices and Microstructures 81 (2015): 193-201.

[21] Hassanien, A. S., and Alaa A. Akl. "Effect of Se addition on optical and electrical properties of chalcogenide CdSSe thin films." Superlattices and Microstructures 89 (2016): 153-169.

[22] Srivastava, Bhupendra B., Santanu Jana, and Narayan Pradhan. "Doping Cu in semiconductor nanocrystals: some old and some new physical insights." Journal of the American Chemical Society 133, no. 4 (2010): 1007-1015.